Original Research

CRISPR/SaCas9-based gene editing rescues photoreceptor degeneration throughout a rhodopsin-associated autosomal dominant retinitis pigmentosa mouse model

Wei Du[1,2,3,4], Jiarui Li[1,2,3,4], Xin Tang[1,2,3,4], Wenzhen Yu[1,2,3,4] and Mingwei Zhao[1,2,3,4]

[1]Department of Ophthalmology and Clinical Centre of Optometry, Peking University People's Hospital, Beijing 100044, China; [2]Eye Diseases and Optometry Institute, Peking University People's Hospital, Beijing 100044, China; [3]Beijing Key Laboratory of Diagnosis and Therapy of Retinal and Choroid Diseases, Beijing 100044, China; [4]College of Optometry, Peking University Health Science Center, Beijing 100044, China
Corresponding author: Wei Du. Email: duwei.o@163.com

Impact Statement

The rhodopsin (*Rho*) gene mutation is frequently found in autosomal dominant retinitis pigmentosa (ADRP); however, effective treatments for ADRP are still required. Therefore, we developed a CRISPR/SaCas9-mediated mutation-independent editing approach in which the toxic mutated rhodopsin is ablated and a healthy variant of the gene is delivered into photoreceptor cells utilizing two separate adeno-associated virus (AAV) vectors *in vivo* throughout the ADRP transgenic mouse model. Following the subretinal injection of the aforementioned "reduction and replacement" system into *Rho*-P23H transgenic mice, mutant rhodopsin expression was reduced and retinal function was improved. Our study provides evidence that the CRISPR/SaCas9-mediated "reduction and replacement" gene editing approach specifically targets the *Rho* gene mutant in *Rho*-P23H knock-in mice, thereby rescuing retinal structure and function. Moreover, with further development, this "reduction and replacement" genome-editing strategy may be applicable to the intervention of other gain-of-function genetic disorders.

Abstract

Rhodopsin (*Rho*) gene mutation was considered the highest prevalent mutation in autosomal dominant retinitis pigmentosa (ADRP); however, effective therapeutics for ADRP have not been developed. The process of gene editing via the clustered regularly interspaced short palindromic repeat (CRISPR)/Cas9 system offers the potentiality to provide cures for dominantly inherited disorders. Herein, we generated a CRISPR/SaCas9-mediated gene reduction system to inactivate the *Rho* mutant, while replacing normal rhodopsin in a rhodopsin mutation mouse model. When *Rho*-P23H knock-in mice were administered a subretinal injection of the "reduction and replacement" system, the expression of mutant rhodopsin was reduced, and retinal function was improved. Therefore, we concluded that CRISPR/SaCas9-based "reduction and replacement" gene therapy could provide structural and functional benefits for *Rho* mutant ADRP, as well as new directions for future clinical research on the treatment of such gain-of-function genetic diseases.

Keywords: Retinitis pigmentosa, rhodopsin, CRISPR/SaCas9, gene therapy

Experimental Biology and Medicine **2023; 248: 1818–1828. DOI: 10.1177/15353702231199069**

Introduction

Retinitis pigmentosa (RP) is distinguished by the gradual deterioration of rod-cone photoreceptors, resulting in the development of nyctalopia and the gradual deterioration of visual function.[1] The genetic variations of RP, including autosomal dominant retinitis pigmentosa (ADRP), autosomal recessive retinitis pigmentosa (ARRP), X-linked RP, and simplex RP (inheritance not known) are caused by over than 100 genetic loci within over than 60 genes. Relatively many genes involved, but the *Rhodopsin* (*Rho*) gene causes 25% of retinal degenerations and 15% of ADRPs.[2,3]

Currently, gene augmentation or replacement therapy has been proven effective in treating ARRP and has shown clinical benefit,[4,5] while it is powerless to ADRP. The treatment techniques now employed for addressing ADRPs are often ineffective for cases with gain-of-function mutations, as these alterations necessitate the silence of the mutant genes in order to achieve functional rescue.

In some studies, the mutant protein was eliminated, which presented its own set of limitations. For example, some studies used ribozyme, RNA interference (RNAi), and zinc finger–based techniques to silence or delete the mutation, and then supplied normal RNA via an ectogenic wild-type transgene.[6–9] Although the results of these studies were encouraging, the sustainability of the treatment and regulating normal gene expression remain challenges that must be overcome to facilitate widespread use of this therapy.

The clustered regularly interspaced short palindromic repeat (CRISPR)/Cas9 system is a specific and stable gene editing technique that can be used to disrupt mutant genes via selective allele targeting. Indeed, the CRISPR/Cas9 system exhibited the ability to be utilized for gene editing in different hosts, including plants, zebrafish, mice, monkeys, and humans.[10–15] The greatest commonly employed Cas9 enzyme is that of *Streptococcus pyogenes* (SpCas9), although its large size restricts its application in adeno-associated virus (AAV)–promoted gene therapy. As CRISPR/Cas9 technology has developed, several smaller Cas9 enzymes from other bacterial species have received attention for their feasibility for use in viral gene therapy, particularly that of *Staphylococcus aureus* (SaCas9).[16] Indeed, SaCas9 is suitable as an AAV delivery vehicle owing to its small size, and the AAV-CRISPR/SaCas9 system has been applied successfully in several gene knockout animal models.[17,18]

Consequently, we choose to utilize the enhanced genome-editing capability of CRISPR/SaCas9 in order to achieve the efficient silencing of the rhodopsin mutation, thereby mitigating photoreceptor deterioration and halting the progression of associated diseases. We designed a two-pronged "reduction and replacement" strategy to reduce mutant *Rho* gene expression utilizing the CRISPR/SaCas9-based gene system and allow normal *Rho* to restore photoreceptor function. Specifically, we used one vector expressing CRISPR/SaCas9-mediated *Rho* gene reduction, and another vector with the single guide RNA (sgRNA)–resistant *Rho* gene expressed in the corresponding knockdown background. We postulate that this strategy could be applicable to rhodopsin-related ADRP and other dominant diseases.

Materials and methods

Animal model

This study followed the protocols outlined in the National Institute of Health Guide for the Care and Use of Laboratory Animals, as well as the Association for Research in Vision and Ophthalmology Statement for the Use of Animals in Ophthalmic and Vision Research. The animal procedures followed the instructions outlined in the Institutional Animal Care and Use Committee of Peking University People's Hospital (permit number: 2016PHC059). $Rho^{P23H/P23H}$ (B6.129S6 (Cg)-Rho tm1.1Kpal/J) mice were acquired from Jackson Laboratories (Bar Harbor, ME, USA; stock no. 017628), while the C57BL/6J mice have been purchased from Beijing Vital River Laboratory Animal Technology Co., Ltd. (Beijing, China). Heterozygous ($Rho^{P23H/+}$) mice have been produced through crossing P23H homozygous ($Rho^{P23H/P23H}$) mice with C57BL/6J wild-type mice. The animals were subjected to a 12/12-h light/dark cycle and were provided with unrestricted access to food and water. For every experiment conducted and at every designated time interval within the experiment, a total of three mice were utilized for each group.

Vector generation and viral production

The sgRNA used in this study was designed using an online sgRNA designer tool (http://crispor.tefor.net/). The sgRNAs exhibiting the most favorable on-targeting scores were selected for experimental evaluation in the present investigation. The sgRNAs with the highest cleavage efficiencies that were also in proximity to the target site were selected for genome editing. The sgRNA sequence (PAM is underlined) was ATTCACCACCACCCTCTACACATCACTC.

For the production of AAV-overexpressing sgRNA-resistant rhodopsin, a 472 bp (−385 to +86) murine rhodopsin promoter (mOP) was used to modulate *Rho* specifically in photoreceptors (Figure 1(f)).[19] The *Rho* (sgRNA-resistant) overexpression vector was FLAG-tagged. These two AAV vectors were packaged with serotype 9 (AAV9) separately, which has been shown to transduce mouse photoreceptors efficiently,[19,20] and were generated by Beijing Corregene Co., Ltd. (Beijing, China).

Synonymous mutations were generated in the sgRNA target sequence to avoid cleavage of the *Rho* overexpression plasmid by the CRISPR/SaCas9 machinery. *Rho* could be expressed even in the presence of sgRNA. The sgRNA-resistant mutant sequence was CTTTACGACGACGCTGTATACTTCTCTC. All primers are presented in Supplementary Table S1.

Cell cultivation and plasmid transfection

The NIH/3T3 cell line (1101MOU-PUMC000018) has been acquired from the National Infrastructure of Cell Line Resource (NICR, Beijing, China). Mycoplasma contamination was assessed on a monthly basis for all cells, and only those cells found to be free of mycoplasma contamination were utilized for investigations. The possible mycoplasma contamination was excluded by the mycoplasma contamination detection kit (CA 1080, Solarbio, Beijing, China). The cells underwent cultivation within a six-well plate at a density of 1×10^6 cells/well. Once the cells achieved a confluency of 75%, the plasmids were introduced into 3T3 cells through transfection utilizing Lipofectamine 3000 (Invitrogen, Carlsbad, CA, USA). The cell culture underwent additional purification using puromycin selection at 2 μg/mL, beginning 48 h subsequent to the transfection process. The isolation of DNA was conducted following a period of two weeks.

Polymerase chain reaction amplicons and T7 endonuclease I analysis

Genomic polymerase chain reaction (PCR) was carried out using Platinum SuperFi II DNA Polymerase (Invitrogen), and the primers utilized for detecting gene truncation are presented in Supplementary Table S1. For T7 endonuclease I (T7EI) analysis, purified PCR products (D2500-01, E.Z.N.A. Gel Extraction Kit, Norcross, GA, USA) were denatured and

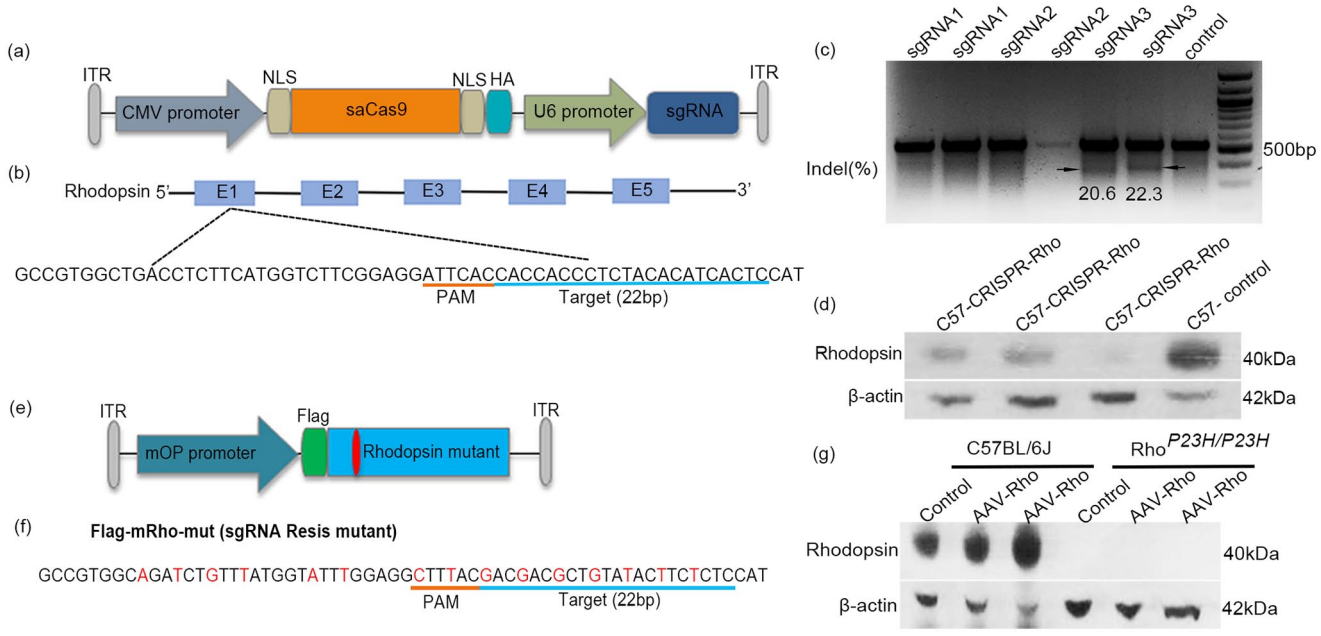

Figure 1. Establishment of the rhodopsin-specific knockdown and re-expression system. (a) Schematic of the plasmid for expressing both SaCas9 and corresponding sgRNA; (b) CRISPR/SaCas9 target sequences and protospacer adjacent motif (PAM) sequences, PAM sequence was underlined; (c) representative gel image of gRNAs editing activity using the T7EI assay; (d) western blot analysis of rhodopsin expression level in C57BL/6J mouse eye after subretinal injection of AAV9-CRISPR/SaCas9-Rho-sgRNA virus; (e) schematic of the plasmid for sgRNA-resistant rhodopsin gene of wild-type, along with FLAG-tag; (f) the sgRNA resists mutant sequence, PAM sequence is underlined, red bases stood for synonymous mutations; (g) western blot analysis of rhodopsin expression level in C57BL/6J mouse and $Rho^{P23H/P23H}$ mouse eyes after subretinal injection of AAV9-mOP-mRho-Flag virus.

reannealed using T7EI (M0302S, NEB, Ipswich, MA, USA) following the guidelines provided by the manufacturer and then analyzed on 2% agarose gels. As mentioned above, the sgRNAs with the highest cleavage efficiency that were in proximity to the target site were selected for genome editing.

Subretinal injection

Subretinal (SR) injections were performed utilizing a 33-gauge blunt needle attached to a 5-μL microsyringe (Hamilton Co., Reno, NV, USA). The injections were administered employing a surgical microscope (OMS-800, TOPCON, Tokyo, Japan) at postnatal day 7 (P7) in the eyes of $Rho^{P23H/P23H}$ and $Rho^{P23H/+}$ mice. The dilation of the pupils was achieved by administering 1% atropine sulfate ophthalmic gel, manufactured by Xingqi Pharmaceutical Co., Ltd. (Shenyang, China). In addition, 0.5% tropicamide and 0.5% phenylephrine hydrochloride eye drops, produced by Santen Pharmaceutical Co., Ltd. (Osaka, Japan), were also used for this purpose. Mice underwent anesthesia using sodium thiopental (50 g/kg). The SR injection of 1 μL of AAV9-CRISPR/SaCas9-Rho-sgRNA (1.82×10^{13} vg/mL) or 1 μL of AAV9-mOP-mRho-Flag (1.36×10^{13} vg/mL) was administered to the C57BL/6J and $Rho^{P23H/P23H}$ mice right eye at P7, while the left eye was uninjected as a control. Subsequently 1 μL of a 1:1 mixture of AAV9-CRISPR/SaCas9-Rho-sgRNA and AAV9-mOP-mRho-Flag was subretinally injected into one eye of each $Rho^{P23H/P23H}$ and $Rho^{P23H/+}$ mouse, while the other eye was left untreated as a control. After the injections, 1% atropine sulfate ophthalmic gel and dexamethasone ophthalmic ointment (S.A. Alcon-Couvreur N.V., Belgium) and tobramycin were applied to reduce injection-related inflammation.

Deep sequencing analysis

The evaluation of indel frequencies of SaCas9-sgRNA pairs utilized throughout the current investigation was conducted using targeted deep sequencing. The PCR amplicons derived from the target sites in mouse retinas, both treated and untreated, were subjected to next-generation sequencing. Supplementary Table S1 lists the primers utilized for this analysis. A paired-end sequencing analysis was carried out on the data via an Illumina MiSeq platform (San Diego, CA, USA). CRISPResso2 was utilized to conduct an analysis on the data obtained from deep sequencing (version 2.0.27; http://crispresso.rocks/).[21,22]

Electroretinography

Scotopic full-field electroretinography (ERG) responses were analyzed using a Ganzfeld ERG system (Roland Consult Stasche & Finger GmbH, Brandenburg, Germany). ERG was measured at three time points (P7 + 4W, P7 + 8W, and P7 + 16W) for $Rho^{P23H/P23H}$ and $Rho^{P23H/+}$ mouse. Control mice were selected to be age-matched C57BL/6J mice. Prior to experimentation, the mice underwent a period of dark adaptation overnight. Subsequently, the pupils of their eyes were expanded with eye drops that contained 0.5% tropicamide and 0.5% phenylephrine hydrochloride. Following this, the mice underwent anesthesia using sodium thiopental at a dosage of 50 g/kg. Scotopic ERGs, which mainly measures rod function, were documented at a stimulus light intensity of 0.025 cd.s/m^2 (−1.6 log cd.s/m^2) by interstimulus interval of 30 s, and the average of 10 recordings was taken. The amplitudes of the b-wave were determined by

measuring the distance from the major cornea-positive peak to the cornea-negative peak. Recordings were made for five mice in each treatment group.

Histological analysis

Histological analysis was performed using eyes enucleated from $Rho^{P23H/P23H}$ and $Rho^{P23H/+}$ mice at the appropriate time point (P7 + 16W) after SR injection. The eyeballs were thereafter immersed in a 4% paraformaldehyde solution overnight at a temperature of 4°C. The experimental procedure involved the execution of routine dehydration and subsequent paraffin embedding. This process yielded paraffin sections with 5 μm thickness. The retinal slices were next subjected to staining with hematoxylin and eosin. Moreover, the resulting slices have been visually documented utilizing an Olympus microscope (Olympus, Tokyo, Japan). The thickness of the outer nuclear layer (ONL) was measured at regular intervals of 50 m, ranging from the optic nerve to both the superior and inferior regions of the retina. The range of this measurement was from the optic nerve to the superior and inferior regions of the retina. A total of five sections from distinct animals within each group were subjected to analysis.

Western blot

Eyeballs were extracted from mice in each group at each time point. The retina samples were subsequently combined and underwent homogenization within radioimmunoprecipitation assay buffer (RIPA) buffer (Solarbio, Beijing, China) containing Protease Inhibitor Cocktail (Roche, Basel, Switzerland) while being kept at a low temperature. Utilizing a modified bicinchoninic acid (BCA) assay, the concentrations of total proteins were determined. The retinal proteins underwent separation using electrophoresis on a 10% Bis-Tris gel (Invitrogen). Subsequently, they were moved onto nitrocellulose membranes and subjected to incubation utilizing a primary antibody specific to rhodopsin. Prior to this step, the membranes underwent inhibition utilizing a solution of 5% defatted milk in Tris-buffered saline with Tween 20 (TBS-T) and kept at a temperature of 4°C overnight. Rhodopsin mouse monoclonal antibody (1:500, ab5417; Abcam, Cambridge, UK) was used to detect rhodopsin. DYKDDDDK tagged mouse monoclonal antibody (1:1000, 66008-3-Ig; Proteintech, Rosemont, IL, USA) was used to detect FLAG-tagged epitopes. Horseradish peroxidase (HRP)–conjugated goat antimouse (1:10000, SA00001-2; Proteintech) detected the primary antibody. X-ray photographic film imaging was used to acquire the densitometry data. Density was normalized to β-actin (1:10000, 66009-1-Ig; Proteintech) and glyceraldehyde 3-phosphate dehydrogenase (GAPDH) (1:10000, 22616, 22619; Thermo Fisher Scientific, Waltham, MA, USA).

Retina frozen section and whole mount preparation

In order to perform frozen section analysis, the eyes were enucleated at designated time intervals subsequent to injection. These enucleated eyes were then fixed inside a 4% paraformaldehyde solution for a duration of 30 min. Subsequently, the cornea and lens were extracted from the ocular structure while ensuring the preservation of the retina's integrity. The eyecups were subsequently incubated for an additional 2 h at room temperature, subsequent by rinsing with phosphate-buffered saline (PBS). To ensure preservation during cryopreservation, the eyecups were then treated with a 30% sucrose/PBS solution at room temperature for a duration of 3 h. Subsequently, the eyecups were immersed in an appropriate cutting temperature compound (Tissue-Tek; Sakura Finetek USA, Inc., Torrance, CA, USA) and subjected to freezing at a temperature of −80°C. The retinas have been sectioned in a dorsal-to-ventral orientation with a thickness of 8 μm. To prepare the whole mount samples, the eyes were meticulously extracted and thereafter immersed in a solution containing 4% paraformaldehyde for a duration of 10 min. Subsequently, the corneas, lenses, vitreous, and retinal pigment epithelia were meticulously extracted. The retinas were then treated to an additional fixation step in a 4% paraformaldehyde solution for a period of 1 h. Following this, the retinas were thoroughly washed with PBS and subsequently subjected to immunofluorescence labeling. Following immunofluorescence labeling, the retinas were divided through the implementation of four radial incisions within the superior, inferior, nasal, and temporal quadrants. The photographs were captured with an Olympus fluorescence microscope manufactured by Olympus. Image-Pro Plus (Media Cybernetics, Silver Spring, MD, USA) has been employed to determine what proportion of the area displayed a positive rhodopsin signal.

Immunofluorescence staining

In the frozen section analysis, the retinal slices were subjected to labeling using biotinylated peanut agglutinin (1:200, B-1075; Vector Laboratories, Burlingame, CA, USA) and rhodopsin antibody (1:100, ab5417; Abcam) at a temperature of 4°C overnight. Subsequently, the sections were subjected to three washes with PBS, underwent incubation with Fluorescein Avidin D (1:500, A-2001; Vector Laboratories) and immunoglobulin G secondary antibody tagged with Alexa-594 (1:500, A11032; Invitrogen) for a duration of 1 h at room temperature, followed by washing by PBS. The mounting of the slices has been then performed by Vectashield® HardSet™ Mounting Medium for Fluorescence (H-1400, Vector Labs, Inc., Burlingame, CA, USA) and cover slipped. Finally, the slices underwent imaging via an Olympus fluorescence microscope (Olympus).

In the case of whole mount samples, the procedures for primary and secondary detection were conducted in a manner similar to those of frozen sections, with the exception that a solution of PBS containing 1% Triton X-100 was utilized. Subsequently, the retinas were subjected to a thorough rinsing process using PBS, followed by their placement onto slides and subsequent application of antifluorescence quencher mounting fluid as a covering.

Statistical analysis

All experiments were conducted with a minimum of three times, and data are expressed as mean values ± standard deviations. In order to identify variations among the various

time periods, one-way analysis of variance (ANOVA) and Bonferroni post hoc tests were utilized. The statistical analysis was performed and graphs were generated utilizing GraphPad Prism version 5 (GraphPad Software, Inc., La Jolla, CA, USA). $P < 0.05$ was reported as statistically significant.

Results

Design of sgRNA for targeting rhodopsin is efficient and viable

To develop CRISPR/SaCas9 gene excision tools, we formulated sgRNAs that were designed to target the first exon of the mouse *Rho* gene, and then cloned these sgRNAs into the pAAV-CMV-SaCas9-U6-sgRNA vector (Figure 1(a) and (b)). In order to assess the *in vitro* editing efficacy of the sgRNAs, we performed transfection investigations by introducing the corresponding plasmids into 3T3 fibroblasts. Following a 14-day period of puromycin determination, the entirety of the genomic DNA was collected for the purpose of conducting PCR. Subsequently, a T7E1 assay was employed to approximate the efficacy of genome editing. Of the sgRNAs, sgRNA3, with an indel efficiency of ~20%, exhibited better ability to form indels than either sgRNA1 or sgRNA2 (Figure 1(c)).

"Reduction and replacement" strategy edits mutant *Rho* effectively *in vivo*

To test the CRISPR/SaCas9-mediated "reduction and replacement" approach *in vivo*, we cloned each component into two AAV9 vectors. CRISPR/SaCas9 and sgRNA expression cassettes regulated by the CMV modulator were combined into one vector (AAV9-CRISPR/SaCas9-Rho-sgRNA), while the sgRNA-resistant mouse RHO (mRHO) complementary DNA (cDNA) (for gene replacement) regulated by mOP was cloned into another vector (AAV9-mOP-mRho-Flag) (Figure 1(e) and (f)).

To validate the ability of AAV9-CRISPR/SaCas9-Rho-sgRNA to mediate gene ablation *in vivo*, a 1-μL SR injection was administered to the adult wild-type C57BL/6J mice (P63) right eye, while the left eye was not labeled as a negative control. Retinal samples were taken for analysis two weeks postinjection. Western blot results indicated that rhodopsin protein levels were significantly decreased by the AAV9-CRISPR/SaCas9-Rho-sgRNA injected into the retinas of C57BL/6J mice (Figure 1(d)). Thus, the selected Rho-sgRNA worked effectively with the CRISPR/SaCas9 system *in vivo*, indicating successful *Rho* ablation.

To verify the ability of the AAV9-mOP-mRho-Flag vector to overexpress the *Rho* gene, AAV9-mOP-mRho-Flag has been inoculated to the adult C57BL/6J (P63) right eye and $Rho^{P23H/P23H}$ mice (P63) (Figure 1(e) and (f)), while the left eye was left unlabeled to serve as a control. The eyes were subjected to analysis two weeks postinjection. Western blot analysis results demonstrated that vector treatment in the eyes of C57BL/6J mice led to an upregulation of the rhodopsin expression level relative to that of untreated eyes, whereas rhodopsin expression was not detected in either treated or untreated eyes of $Rho^{P23H/P23H}$ mice (Figure 1(g)). This result suggests that the AAV9-mOP-mRho-Flag vector successfully induces rhodopsin protein overexpress after SR injection in C57BL/6J mice. However, in $Rho^{P23H/P23H}$ mice, because the P23H mutation results in dominant gain-of-function, normal rhodopsin was not expressed after injection with the AAV9-mOP-mRho-Flag vector alone.

For the purpose of comparing the gene editing efficiency of single virus (reduction or replacement virus) versus dual viruses (reduction and replacement), 1 μL of AAV9-CRISPR/SaCas9-Rho-sgRNA (1.82×10^{13} vg/mL), or 1 μL of AAV9-mOP-mRho-Flag (1.36×10^{13} vg/mL), or 1 μL of AAV9-CRISPR/SaCas9-Rho-sgRNA and AAV9-mOP-mRho-Flag (1:1) was administered by SR inoculation to $Rho^{P23H/P23H}$ mice right eye at P7, while the left eye was has not inoculated to function as a control. After two weeks, differential expression of rhodopsin has been validated utilizing the western blot. Rhodopsin was not expressed in either the reduction virus only group or replacement virus only group, while rhodopsin expression was detected in the dual virus injection group (Supplementary Figure S1a). This result shows that treatment with either reduction or replacement alone could not elevate rhodopsin expression, whereas dual virus injection could effectively increase the expression level.

To characterize the efficacy of gene editing of the "reduction and replacement" system, we examined the distribution of rhodopsin expression in $Rho^{P23H/P23H}$ mice on retinal whole mount two weeks after dual virus injection. On retinal whole mount, approximately 30% of retinal cells expressed rhodopsin (Supplementary Figure S2). We also used a deep sequencing analysis to quantify the gene editing efficiency of dual virus injection in $Rho^{P23H/P23H}$ mice. The CRISPResso pipeline analyzed the deep-coverage sequence reads. At two weeks postinjection, the editing efficiency in eyes treated with dual virus was $12.08 \pm 1.25\%$, which exhibit significant elevation ($P < 0.05$) than that of untreated eyes $7.50 \pm 0.18\%$ (Supplementary Figures S3 and S4). These data demonstrate that the "reduction and replacement" system induced efficient editing (Supplementary Table S2).

Mixture of AAV9-CRISPR/SaCas9-Rho-sgRNA and AAV9-mOP-mRho-Flag treatment restores rod function

To compare the rod function recovery of single versus dual virus, the assessment of retinal function was conducted using scotopic full-field ERG. After a duration of four weeks, it was shown that at a stimulus intensity of 0.025 cd.s/m^2, the amplitudes of both a-wave and b-wave showed significant improvements in eyes that were treated with dual viruses, as compared to eyes that were treated with a single virus. The findings of the mean maximum a-wave amplitude of single virus treated eye was 4.90 ± 1.44 μV ($n = 3$) and 3.17 ± 1.15 μV ($n = 3$) and that of dual virus treated eyes was 18.77 ± 2.05 μV ($n = 3$, $P < 0.01$). The outcomes of the mean maximum b-wave amplitude of single virus treated eyes was 4.53 ± 2.29 μV ($n = 3$) and 5.47 ± 1.39 μV ($n = 3$) and that of dual virus treated eyes was 45.73 ± 6.03 μV ($n = 3$, $P < 0.01$) (Supplementary Figure S1B). Rod function was not recovered effectively by single virus injection.

For evaluating the long-term recovery of retinal functionality in eyes treated with dual viruses, scotopic full-field ERG

was performed. For $Rho^{P23H/P23H}$ mice, at a stimulus intensity of 0.025 cd.s/m^2, both a-wave and b-wave amplitudes exhibited significant enhancement for eyes that underwent treatment contrasted to untreated eyes at four weeks, and these improvements were kept for 16 weeks after SR injections of AAV9-CRISPR/SaCas9-Rho-sgRNA and AAV9-mOP-mRho-Flag vector (Figure 2(a)). The mean maximum a-wave amplitude for untreated eyes was $1.76 \pm 0.52\,\mu V$ ($n = 6$), whereas that for treated eyes examined for ERG function at four weeks postinjection (P7 + 4W) was $17.85 \pm 2.57\,\mu V$ ($n = 6$, $P < 0.001$) (Figure 2(b)). The a-wave amplitudes at P7 + 8W and P7 + 16W was $15.33 \pm 2.41\,\mu V$ ($n = 6$, $P < 0.001$) and $11.85 \pm 1.30\,\mu V$ ($n = 6$, $P < 0.01$), respectively (Figure 2(b)). The mean maximum b-wave amplitude for untreated eyes was $3.77 \pm 0.99\,\mu V$ ($n = 6$), while that for treated eyes was $41.27 \pm 8.06\,\mu V$ ($n = 6$, $P < 0.001$) at P7 + 4W, $26.42 \pm 8.67\,\mu V$ ($n = 6$, $P < 0.05$) at P7 + 8W, and $23.70 \pm 11.08\,\mu V$ ($n = 6$, $P < 0.05$) at P7 + 16W (Figure 2(c)).

SR injections of AAV9-CRISPR/SaCas9-Rho-sgRNA and AAV9-mOP-mRho-Flag vector also consistently improved rod function in $Rho^{P23H/+}$ mice. The mean maximum a-wave amplitude for untreated eyes deteriorated compared with that for treated eyes at all time points measured (Figure 2(d)). At P7 + 4W, the mean maximum a-wave amplitude in untreated eyes was $28.32 \pm 5.51\,\mu V$ ($n = 5$), while that for treated eyes was $48.12 \pm 7.72\,\mu V$ ($n = 5$, $P < 0.01$); at P7 + 8W, the mean maximum a-wave amplitude for untreated eyes was $9.76 \pm 2.86\,\mu V$ ($n = 5$) and that for treated eyes was $29.98 \pm 3.85\,\mu V$ ($n = 5$, $P < 0.01$); at P7 + 16W, the mean maximum a-wave amplitude for untreated eyes was $3.88 \pm 0.69\,\mu V$ ($n = 5$), whereas that for treated eyes was $20.14 \pm 1.67\,\mu V$ ($n = 5$, $P < 0.05$) (Figure 2(e)). Similarly, contrasted to treated eyes, the b-wave amplitude of untreated eyes showed significant reduction at P7 + 4W (untreated: $58.56 \pm 5.96\,\mu V$; treated: $90.34 \pm 5.20\,\mu V$; $n = 5$, $P < 0.01$), P7 + 8W (untreated: $22.66 \pm 6.28\,\mu V$; treated: $75.12 \pm 7.51\,\mu V$; $n = 5$, $P < 0.001$), and P7 + 16W (untreated: $9.08 \pm 2.73\,\mu V$; treated: $32.18 \pm 3.75\,\mu V$; $n = 5$, $P < 0.05$) (Figure 2(f)).

Although the scotopic ERG amplitudes for treated eyes declined gradually compared with those at four weeks postinjection, they remained relatively stable from 8 to 16 weeks for $Rho^{P23H/P23H}$ mice, and similar restoration was observed in $Rho^{P23H/+}$ mice from 8 to 16 weeks postinjection.

Combined AAV9-CRISPR/SaCas9-Rho-sgRNA and AAV9-mop-mRho-Flag treatment partially preserves retinal structure

The quantification of the ONL thickness is regarded as a significant parameter for assessing the survival of photoreceptors.[23] The effects of SR injection of combined virus on the retinal structure of $Rho^{P23H/P23H}$ and $Rho^{P23H/+}$ mice were evaluated by comparing the thicknesses of ONL in the superior and inferior retinas of both treated and untreated eyes.

$Rho^{P23H/P23H}$ mice have been observed to have a swift and profound degradation of rod-driven retinal function following birth, leading to the total loss of rods by P35. The inner and outer photoreceptor segment at this age exhibit reduced length, and the ONL demonstrates a thinning effect with 0–1 rows of nuclei.[24] Eyes administered a combined virus injection at P119 (P7 + 16W) revealed a significant enhancement within the retinal morphology by the preservation of 6–7 rows of photoreceptor nuclei; in contrast, the ONL of untreated eye was only a single row at P119 (treated: $19.25 \pm 1.55\,\mu m$ (superior) and $21.16 \pm 1.08\,\mu m$ (inferior); untreated: $4.76 \pm 0.74\,\mu m$ (superior) and $4.73 \pm 0.51\,\mu m$ (inferior); $P < 0.01$, $n = 6$) (Figure 3(a) to (c)). In addition, the inner and outer photoreceptor segment of treated eyes was preserved compared to untreated eyes.

Retinal degeneration in $Rho^{P23H/+}$ mice is dramatically slower than in $Rho^{P23H/P23H}$ mice: severe retinal degeneration was found to develop at P63, and rod death was complete by about 6–10 months.[25] SR injection of AAV9-CRISPR/SaCas9-Rho-sgRNA and AAV9-mOP-mRho-Flag caused a marked effect in $Rho^{P23H/+}$ mice, with the ONL thickness significantly improving across the entire retina at 16 weeks postinjection (P7 + 16W) compared with uninjected eyes (P119) (treated eye: $17.59 \pm 1.17\,\mu m$ (superior) and $19.48 \pm 1.82\,\mu m$ (inferior); untreated eye: $7.13 \pm 1.42\,\mu m$ (superior) and $6.28 \pm 1.04\,\mu m$ (inferior); $P < 0.001$, $n = 6$) (Figure 3(d) to (f)).

Combined AAV9-CRISPR/SaCas9-Rho-sgRNA and AAV9-mOP-mRho-Flag treatment leads to rhodopsin preservation

To determine whether rhodopsin was expressed after injection with two viruses, immunoblotting analysis and immunofluorescence staining were performed. Western blot analysis indicated that rhodopsin was not obviously expressed in untreated $Rho^{P23H/P23H}$ mouse eyes at P35, P63, and P119, whereas vector treatment in mice at P7 + 4W, P7 + 8W, and P7 + 16W led to significantly higher levels of rhodopsin. Rhodopsin levels were also analyzed in $Rho^{P23H/+}$ mouse retinas at the same time points. The rhodopsin protein levels in treated retinas at each time point (P7 + 4W, P7 + 8W, and P7 + 16W) were markedly upregulated relative to untreated retinas (P35, P63, and P119) (Figure 4(a)). Because the sgRNA-resistant rhodopsin overexpression vector carried a FLAG-tag, it was possible to compare the expression levels of wild-type and FLAG-tagged rhodopsin using an appropriate antibody. Probing with FLAG antibody revealed that only subretinally injected eyes contained the FLAG-tag, while uninjected eyes exhibited no FLAG-tag (Figure 4(b)).

Retinal cryosections underwent treatment with an anti-rhodopsin antibody in order to evaluate the viability of rod cells in retinas that had been treated. Age-matched wild-type C57BL/6J mice exhibited strong expression of rhodopsin. In $Rho^{P23H/P23H}$ mice, rhodopsin labeling was observed in injected retinas at P7 + 4W, P7 + 8W, and P7 + 16W, whereas no detectible rhodopsin labeling was found in the contralateral uninjected eyes (P119) (Figure 4(c)). Rhodopsin expression was also detected in $Rho^{P23H/+}$ mouse eyes following combined virus treatment. $Rho^{P23H/+}$ mice exhibit progressive photoreceptor degeneration, and most photoreceptors are absent at four months of age;[26] thus, rhodopsin was detected in both treated and untreated retinas, but its expression levels in treated retinas were much higher than in untreated retinas at P35 (P7 + 4W) and P63 (P7 + 8W). At P119 (P7 + 16W), rhodopsin staining was diffuse in untreated retinas but still present in treated retinas (Figure 4(d)).

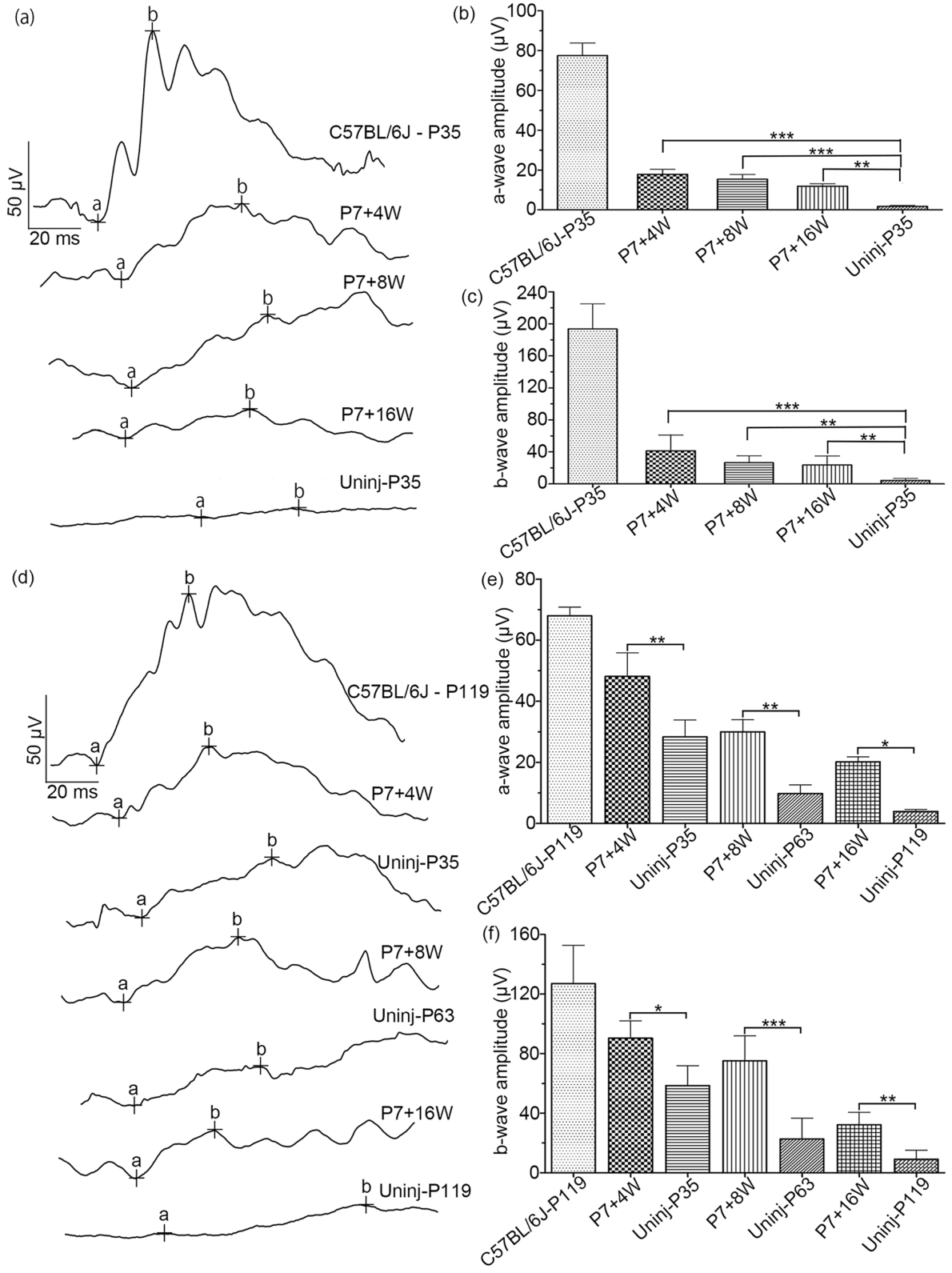

Figure 2. Scotopic electroretinograms (ERGs) and statistical analysis. (a to c) Scotopic electroretinograms (ERGs) and statistical analysis of Rho$^{P23H/P23H}$ mouse: (a) representative scotopic ERG tracings elicited at 0.025 cd.s/m^2 from Rho$^{P23H/P23H}$ and control eyes at 4, 8, and 16 weeks after subretinal injection at P7 and WT controls; (b) average a-wave amplitudes elicited at 0.025 cd.s/m^2 ($n = 6$ in each group); (c) average b-wave amplitudes elicited at 0.025 cd.s/m^2 ($n = 6$ in each group); (d to f) scotopic electroretinograms (ERGs) and statistical analysis of Rho$^{P23H/+}$ mouse: (d) representative scotopic ERG tracings elicited at 0.025 cd.s/m^2 from Rho$^{P23H/+}$ and control eyes at 4, 8, and 16 weeks after subretinal injection at P7 and WT controls; (e) average a-wave amplitudes elicited at 0.025 cd.s/m^2 ($n = 6$ in each group); (f) average b-wave amplitudes elicited at 0.025 cd.s/m^2 ($n = 6$ in each group). All of scotopic ERG scale bars are the same: x-axis: 20 ms/Div, y-axis: 50 µV/Div. Data are expressed as mean values ± SD

P7 + 4W: eye treated at postnatal day 7 with ERG analysis at four weeks after injection; P7 + 8W: eye treated at postnatal day 7 with ERG analysis at eight weeks after injection; P7 + 16W: eye treated at postnatal day 7 with ERG analysis at 16 weeks after injection; Uninj-P35: uninjected eye at 35 days of age; Uninj-P63: uninjected eye at 63 days of age; Uninj-P119: uninjected eye at 119 days of age.

*$P < 0.05$; **$P < 0.001$; ***$P < 0.0001$.

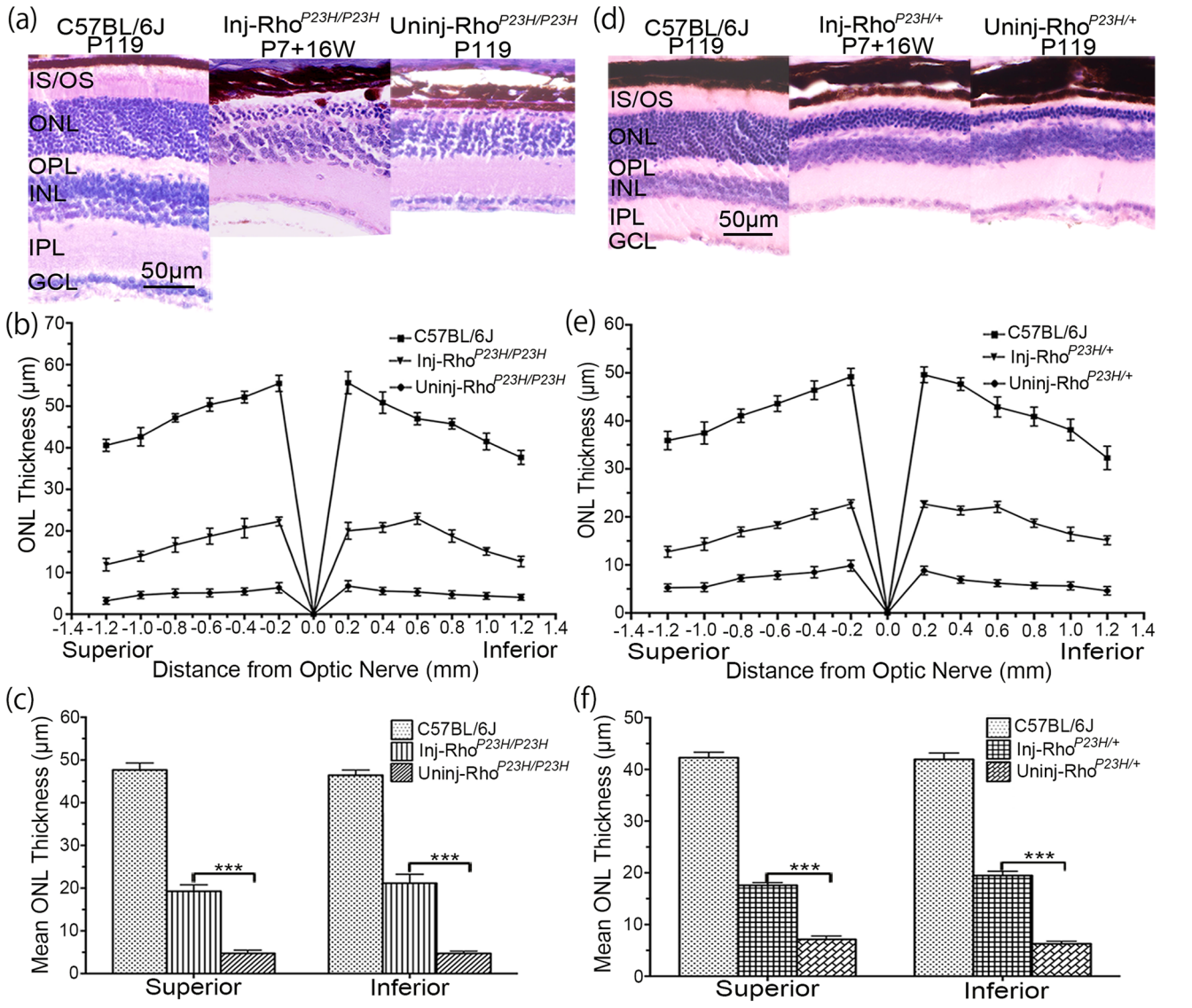

Figure 3. Rescue of retinal structure after treatment. (a) Representative H–E images of retina sections from Rho$^{P23H/P23H}$ and control eyes at 16 weeks after subretinal injection and WT controls; (b) quantification of ONL thickness in the region of 0.2–1.4 mm from the optic nerve to the peripheral retina, and extending every 0.2 mm outward along superior and inferior for Rho$^{P23H/P23H}$ and control eyes at 16 weeks after subretinal injection and WT controls ($n = 5$ in all groups); (c) the mean of the thickness of ONL from the optic nerve to the peripheral retina for Rho$^{P23H/P23H}$ and control eyes at 16 weeks after subretinal injection and WT controls ($n = 5$ in each group); (d) representative H–E images of retina sections from Rho$^{P23H/+}$ and control eyes at 16 weeks after subretinal injection and WT controls; (e) quantification of ONL thickness in the region 0.2–1.4 mm from the optic nerve head to the peripheral retina, and extending every 0.2 mm outward along superior and or inferior for Rho$^{P23H/+}$ and control eyes at 16 weeks after subretinal injection and WT controls ($n = 5$ in each group); (f) the mean of the thickness of ONL from the optic nerve to the peripheral retina for Rho$^{P23H/+}$ and control eyes at 16 weeks after subretinal injection and WT controls ($n = 5$ in each group). Scale bar represents 50 μm. Data are represented at as mean value ± SD.
GCL: ganglion cell layer; IPL: inner plexiform layer; INL: inner nuclear layer; OPL: outer plexiform layer; ONL: outer nuclear layer; OS: outer segment.
***$P < 0.0001$.

Our findings indicated that early intervention has the potential to be occurred in mice, and the treatment effect persists for an extended period after vector injection.

Discussion

Throughout the current investigation, we established a mutation-independent editing technique in which the toxic mutated rhodopsin is ablated, and a healthy variant of the gene is delivered into photoreceptor cells utilizing two separate AAV vectors and tested it *in vivo* across a *Rho*-P23H knock-in mouse model of ADRP. The combined AAV9-CRISPR/SaCas9-Rho-sgRNA and AAV9-mOP-mRho-Flag therapy provided functional rescue in the eyes of both homozygous and heterozygous mice (Figure 2). Four months after treatment, prominent rescue of photoreceptors, represented by a thicker ONL and enhanced expression of rhodopsin, was shown in treated eyes, and visual function was retained to a certain degree (Figures 3 and 4). These findings demonstrate that CRISPR/SaCas9-mediated "reduction and replacement" gene editing therapy can provide favorable efficiency in the ADRP mouse model.

Gene augmentation or gene replacement therapy has long been considered an ideal treatment that provides benefits

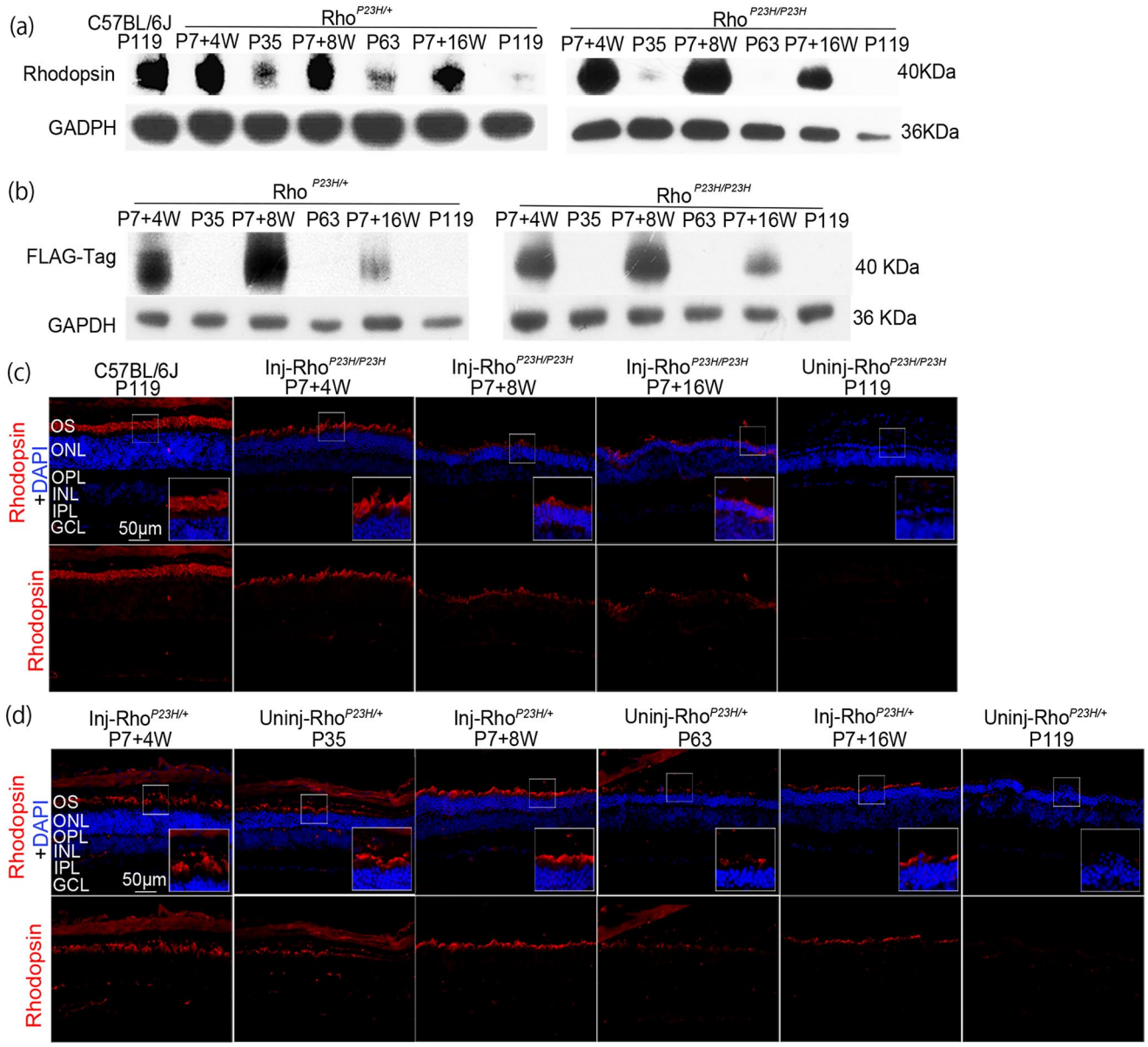

Figure 4. Western blot and immunofluorescence staining analysis of rhodopsin expression. (a) Western blot analysis of rhodopsin expression level in Rho$^{P23H/P23H}$ and Rho$^{P23H/+}$ mice eyes at 4, 8, and 16 weeks after subretinal injection at P7 and wild-type (C57BL/6J) eyes. (b) Western blot analysis of FLAG-tag in treated and untreated eyes at 4, 8, and 16 weeks after subretinal injection at P7. Expression of GAPDH was used as an internal control. (c) Frozen retinal sections immunostaining with antimouse rhodopsin antibody showing rhodopsin expression in OS of Rho$^{P23H/P23H}$ treated eyes at 4, 8, and 16 weeks after subretinal injection and age-matched control C57BL/6J eyes, but not in untreated eyes. (d) In Rho$^{P23H/+}$ mice retinas, rhodopsin can be detected in both treated and untreated retinas at P35 (P7 + 4W) and P63 (P7 + 8W), but the rhodopsin expression level in the treated retinas is much higher than in untreated retinas. At P119 (P7 + 16W), rhodopsin staining was defused in untreated retinas, while in treated retinas, rhodopsin staining was still present. Scale bar represents 50 μm
GCL: ganglion cell layer; IPL: inner plexiform layer; INL: inner nuclear layer; OPL: outer plexiform layer; ONL: outer nuclear layer; OS: outer segment; red: rhodopsin; blue: DAPI.

for patients with inherited retinal dystrophies. However, most ADRPs are excluded from these therapies because of gain-of-function mutations.[27] Despite the inherent complexity of treating ADRP, several research groups have attempted "cut and replace" strategies using RNAi or catalytic RNA enzymes (ribozymes).[28–30] Both siRNA- and ribozyme-based strategies use dose-dependent post-transcriptional interference to temporarily inhibit the expression of RNA, and these treatments are known to elicit off-target effects, instability, and immunogenicity.[31–33] Some other "cut and replace" studies focus on specific mutated alleles;[34,35] these therapies are only suited for specific allele mutation. In contrast to treatments that target specific mutation sites in animal models of severe ADRP, we established the mutation-independent gene editing technique to treat *Rho*-related ADRP irrespective of the mode of a specific allele alteration.

Although a previous study used the reduction and replacement method for the treatment of ADRP, the Cas9 cDNA underwent packaging into one AAV vector, whereas the gRNA expression cassettes and *Rho* cDNA were cloned into another.[23] This approach resulted in a reduction in the overall efficiency of gene editing since it required the

co-infection of cells in order to supply all of the necessary components.[36] In our study, we used a smaller variant Cas9 from SaCas9,[16] which can package SaCas9 cDNA and gRNA into one vector to overcome these existing limitations.

Theoretically, autosomal dominant diseases can only be cured by deleting or correcting the modified allele while leaving the wild-type allele intact.[37] Photoreceptors should be given both suppression and replacement components, and as a result, they should perform similarly to photoreceptors of the wild-type. In a previous study, RNAi-based rhodopsin suppressors and codon-modified rhodopsin replacement genes were delivered by two separate AAVs. It has been shown that co-administration of two AAV vectors (suppression and replacement) results in co-expression of both vector markers in the generality of the transduced cells at the cellular level.[38] We did not observe recovery when mice were treated with a single AAV vector (Supplementary Figure S1). However, compared with the control, dual virus treated eyes were indeed observed the rescue on both expression and function. These results in some extent certified that two different vectors can introduce the genes into the same cells and achieve successful gene editing on target cells after a single SR injection.

Using deep sequencing analysis, we have successfully revealed the possibility of reducing the expression of mutant Rho in the Rho-P23H knock-in mouse model (Supplementary Figures S2 and S3). Studies have confirmed that the CRISPR/Cas9 system stimulates DNA double-strand breakdown, which stimulate the nonhomologous end-joining (NHEJ) DNA repair mechanism that corrects the DNA insult. The induction of frameshifts and the elimination of mutant alleles can be achieved by the utilization of small insertions and deletions facilitated by NHEJ.[16,39] Compared with a previous study on editing efficiency conducted *in vitro*,[40] we found that the prevalence of indels demonstrated a reduced knockdown efficiency than that observed *in vitro*, which was probably as a result of the diluted viral titer caused by the combination of two viruses and the lower copy number of combined plasmids performed *in vivo*.[41] Notably, a low level of mutant Rho transcriptional repression was sufficient to mitigate the degeneration of photoreceptor within mouse and pig models.[6,42] This limitation could be overcome using a relevant and effective *in vivo* delivery approach, for example, enhancing sgRNA targeting efficiency by combining two sgRNAs in a single AAV vector.

In summary, our study demonstrates that the CRISPR/SaCas9-mediated "reduction and replacement" strategy can provide structural and functional benefit for *Rho* mutant ADRP in *Rho* knock-in mice. The results present in our study may also provide some new directions for future clinical research on the treatment of such gain-of-function genetic diseases.

AUTHORS' CONTRIBUTIONS

WD conceived and designed the investigations, evaluated the data, and authored the manuscript. JL and XT conducted the investigations. WY and MZ involved in the manuscript revision. Each author has reviewed and approved the final version of the manuscript.

DECLARATION OF CONFLICTING INTERESTS

The author(s) declared no potential conflicts of interest with respect to the research, authorship, and/or publication of this article.

FUNDING

The author(s) disclosed receipt of the following financial support for the research, authorship, and/or publication of this article: The research conducted in this study received financial assistance from the National Natural Science Foundation of China (grant no. 81600770) and the Beijing Municipal Natural Science Foundation (grant no. 7164306).

ORCID ID

Wei Du https://orcid.org/0000-0001-7953-2023

SUPPLEMENTAL MATERIAL

Supplemental material for this article is available online.

REFERENCES

1. Hartong DT, Berson EL, Dryja TP. Retinitis pigmentosa. *Lancet* 2006;**368**:1795–809
2. Iannaccone A, Man D, Waseem N, Jennings BJ, Ganapathiraju M, Gallaher K, Reese E, Bhattacharya SS, Klein-Seetharaman J. Retinitis pigmentosa associated with rhodopsin mutations: correlation between phenotypic variability and molecular effects. *Vision Res* 2006;**46**:4556–67
3. Dryja TP, McGee TL, Hahn LB, Cowley GS, Olsson JE, Reichel E, Sandberg MA, Berson EL. Mutations within the rhodopsin gene in patients with autosomal dominant retinitis pigmentosa. *N Engl J Med* 1990;**323**:1302–7
4. MacLaren RE, Groppe M, Barnard AR, Cottriall CL, Tolmachova T, Seymour L, Clark KR, During MJ, Cremers FP, Black GC, Lotery AJ, Downes SM, Webster AR, Seabra MC. Retinal gene therapy in patients with choroideremia: initial findings from a phase 1/2 clinical trial. *Lancet* 2014;**383**:1129–37
5. Boye SE, Boye SL, Lewin AS, Hauswirth WW. A comprehensive review of retinal gene therapy. *Mol Ther* 2013;**21**:509–19
6. Mussolino C, Sanges D, Marrocco E, Bonetti C, Di Vicino U, Marigo V, Auricchio A, Meroni G, Surace EM. Zinc-finger-based transcriptional repression of rhodopsin in a model of dominant retinitis pigmentosa. *EMBO Mol Med* 2011;**3**:118–28
7. Jiang L, Zhang H, Dizhoor AM, Boye SE, Hauswirth WW, Frederick JM, Baehr W. Long-term RNA interference gene therapy in a dominant retinitis pigmentosa mouse model. *Proc Natl Acad Sci U S A* 2011;**108**:18476–81
8. LaVail MM, Yasumura D, Matthes MT, Drenser KA, Flannery JG, Lewin AS, Hauswirth WW. Ribozyme rescue of photoreceptor cells in P23H transgenic rats: long-term survival and late-stage therapy. *Proc Natl Acad Sci USA* 2000;**97**:11488–93
9. Lewin AS, Drenser KA, Hauswirth WW, Nishikawa S, Yasumura D, Flannery JG, LaVail MM. Ribozyme rescue of photoreceptor cells in a transgenic rat model of autosomal dominant retinitis pigmentosa. *Nat Med* 1998;**4**:967–71
10. Niu Y, Shen B, Cui Y, Chen Y, Wang J, Wang L, Kang Y, Zhao X, Si W, Li W, Xiang AP, Zhou J, Guo X, Bi Y, Si C, Hu B, Dong G, Wang H, Zhou Z, Li T, Tan T, Pu X, Wang F, Ji S, Zhou Q, Huang X, Ji W, Sha J. Generation of gene-modified cynomolgus monkey via Cas9/RNA-mediated gene targeting in one-cell embryos. *Cell* 2014;**156**:836–43
11. Day TP, Byrne LC, Schaffer DV, Flannery JG. Advances in AAV vector development for gene therapy in the retina. *Adv Exp Med Biol* 2014;**801**:687–93

12. Wang H, Yang H, Shivalila CS, Dawlaty MM, Cheng AW, Zhang F, Jaenisch R. One-step generation of mice carrying mutations in multiple genes by CRISPR/Cas-mediated genome engineering. *Cell* 2013;**153**:910–8
13. Mali P, Yang L, Esvelt KM, Aach J, Guell M, DiCarlo JE, Norville JE, Church GM. RNA-guided human genome engineering via Cas9. *Science* 2013;**339**:823–6
14. Li JF, Norville JE, Aach J, McCormack M, Zhang D, Bush J, Church GM, Sheen J. Multiplex and homologous recombination-mediated genome editing in Arabidopsis and Nicotiana benthamiana using guide RNA and Cas9. *Nat Biotechnol* 2013;**31**:688–91
15. Hwang WY, Fu Y, Reyon D, Maeder ML, Tsai SQ, Sander JD, Peterson RT, Yeh JR, Joung JK. Efficient genome editing in zebrafish using a CRISPR-Cas system. *Nat Biotechnol* 2013;**31**:227–9
16. Ran FA, Cong L, Yan WX, Scott DA, Gootenberg JS, Kriz AJ, Zetsche B, Shalem O, Wu X, Makarova KS, Koonin EV, Sharp PA, Zhang F. *In vivo* genome editing using *Staphylococcus aureus* Cas9. *Nature* 2015;**520**:186–91
17. Zuris JA, Thompson DB, Shu Y, Guilinger JP, Bessen JL, Hu JH, Maeder ML, Joung JK, Chen ZY, Liu DR. Cationic lipid-mediated delivery of proteins enables efficient protein-based genome editing *in vitro* and *in vivo*. *Nat Biotechnol* 2015;**33**:73–80
18. Swiech L, Heidenreich M, Banerjee A, Habib N, Li Y, Trombetta J, Sur M, Zhang F. *In vivo* interrogation of gene function in the mammalian brain using CRISPR-Cas9. *Nat Biotechnol* 2015;**33**:102–6
19. Dalkara D, Byrne LC, Lee T, Hoffmann NV, Schaffer DV, Flannery JG. Enhanced gene delivery to the neonatal retina through systemic administration of tyrosine-mutated AAV9. *Gene Ther* 2012;**19**:176–81
20. Flannery JG, Zolotukhin S, Vaquero MI, LaVail MM, Muzyczka N, Hauswirth WW. Efficient photoreceptor-targeted gene expression *in vivo* by recombinant adeno-associated virus. *Proc Natl Acad Sci USA* 1997;**94**:6916–21
21. Canver MC, Haeussler M, Bauer DE, Orkin SH, Sanjana NE, Shalem O, Yuan GC, Zhang F, Concordet JP, Pinello L. Integrated design, execution, and analysis of arrayed and pooled CRISPR genome-editing experiments. *Nat Protoc* 2018;**13**:946–86
22. Pinello L, Canver MC, Hoban MD, Orkin SH, Kohn DB, Bauer DE, Yuan GC. Analyzing CRISPR genome-editing experiments with CRISPResso. *Nat Biotechnol* 2016;**34**:695–7
23. Michon JJ, Li ZL, Shioura N, Anderson RJ, Tso MO. A comparative study of methods of photoreceptor morphometry. *Invest Ophthalmol Vis Sci* 1991;**32**:280–4
24. Sakami S, Maeda T, Bereta G, Okano K, Golczak M, Sumaroka A, Roman AJ, Cideciyan AV, Jacobson SG, Palczewski K. Probing mechanisms of photoreceptor degeneration in a new mouse model of the common form of autosomal dominant retinitis pigmentosa due to P23H opsin mutations. *J Biol Chem* 2011;**286**:10551–67
25. Tsai YT, Wu WH, Lee TT, Wu WP, Xu CL, Park KS, Cui X, Justus S, Lin CS, Jauregui R, Su PY, Tsang SH. Clustered regularly interspaced short palindromic repeats-based genome surgery for the treatment of autosomal dominant retinitis pigmentosa. *Ophthalmology* 2018;**125**:1421–30
26. Sakami S, Kolesnikov AV, Kefalov VJ, Palczewski K. P23H opsin knock-in mice reveal a novel step in retinal rod disc morphogenesis. *Hum Mol Genet* 2014;**23**:1723–41
27. Lewin AS, Rossmiller B, Mao H. Gene augmentation for adRP mutations in RHO. *Cold Spring Harb Perspect Med* 2014;**4**:a017400
28. Gorbatyuk M, Justilien V, Liu J, Hauswirth WW, Lewin AS. Preservation of photoreceptor morphology and function in P23H rats using an allele independent ribozyme. *Exp Eye Res* 2007;**84**:44–52
29. Kiang AS, Palfi A, Ader M, Kenna PF, Millington-Ward S, Clark G, Kennan A, O'reilly M, Tam LC, Aherne A, McNally N, Humphries P, Farrar GJ. Toward a gene therapy for dominant disease: validation of an RNA interference-based mutation-independent approach. *Mol Ther* 2005;**12**:555–61
30. Cashman SM, Binkley EA, Kumar-Singh R. Towards mutation-independent silencing of genes involved in retinal degeneration by RNA interference. *Gene Ther* 2005;**12**:1223–8
31. Lam JK, Chow MY, Zhang Y, Leung SW. siRNA versus miRNA as therapeutics for gene silencing. *Mol Ther Nucleic Acids* 2015;**4**:e252
32. Pecot CV, Calin GA, Coleman RL, Lopez-Berestein G, Sood AK. RNA interference in the clinic: challenges and future directions. *Nat Rev Cancer* 2011;**11**:59–67
33. Jackson AL, Linsley PS. Recognizing and avoiding siRNA off-target effects for target identification and therapeutic application. *Nat Rev Drug Discov* 2010;**9**:57–67
34. Li P, Kleinstiver BP, Leon MY, Prew MS, Navarro-Gomez D, Greenwald SH, Pierce EA, Joung JK, Liu Q. Allele-specific CRISPR-Cas9 genome editing of the single-base P23H mutation for rhodopsin-associated dominant retinitis pigmentosa. *CRISPR J* 2018;**1**:55–64
35. Bakondi B, Lv W, Lu B, Jones MK, Tsai Y, Kim KJ, Levy R, Akhtar AA, Breunig JJ, Svendsen CN, Wang S. *In vivo* CRISPR/Cas9 gene editing corrects retinal dystrophy in the S334ter-3 rat model of autosomal dominant retinitis pigmentosa. *Mol Ther* 2016;**24**:556–63
36. Vagni P, Perlini LE, Chenais NAL, Marchetti T, Parrini M, Contestabile A, Cancedda L, Ghezzi D. Gene editing preserves visual functions in a mouse model of retinal degeneration. *Front Neurosci* 2019;**13**:945
37. Dalkara D, Goureau O, Marazova K, Sahel JA. Let there be light: gene and cell therapy for blindness. *Hum Gene Ther* 2016;**27**:134–47
38. Millington-Ward S, Chadderton N, O'Reilly M, Palfi A, Goldmann T, Kilty C, Humphries M, Wolfrum U, Bennett J, Humphries P, Kenna PF, Farrar GJ. Suppression and replacement gene therapy for autosomal dominant disease in a murine model of dominant retinitis pigmentosa. *Mol Ther* 2011;**19**:642–9
39. Ousterout DG, Kabadi AM, Thakore PI, Majoros WH, Reddy TE, Gersbach CA. Multiplex CRISPR/Cas9-based genome editing for correction of dystrophin mutations that cause Duchenne muscular dystrophy. *Nat Commun* 2015;**6**:6244
40. Latella MC, Di Salvo MT, Cocchiarella F, Benati D, Grisendi G, Comitato A, Marigo V, Recchia A. *In vivo* editing of the human mutant rhodopsin gene by electroporation of plasmid-based CRISPR/Cas9 in the mouse retina. *Mol Ther Nucleic Acids* 2016;**5**:e389
41. Nelson CE, Hakim CH, Ousterout DG, Thakore PI, Moreb EA, Castellanos Rivera RM, Madhavan S, Pan X, Ran FA, Yan WX, Asokan A, Zhang F, Duan D, Gersbach CA. *In vivo* genome editing improves muscle function in a mouse model of Duchenne muscular dystrophy. *Science* 2016;**351**:403–7
42. Botta S, Marrocco E, de Prisco N, Curion F, Renda M, Sofia M, Lupo M, Carissimo A, Bacci ML, Gesualdo C, Rossi S, Simonelli F, Surace EM. Rhodopsin targeted transcriptional silencing by DNA-binding. *eLife* 2016;**5**:e12242

(Received May 11, 2023, Accepted August 12, 2023)